SCIENCE CHINA
Information Sciences

June 2024, Vol. 67, Iss. 6, 160406:1–160406:7
https://doi.org/10.1007/s11432-024-4032-6

• RESEARCH PAPER •
Special Topic: Silicon-compatible 2D Materials Technologies

Hole mobility enhancement in monolayer WSe_2 p-type transistors through molecular doping

Shiyuan LIU[1], Xiong XIONG[1,2*], Xin WANG[2], Xinhang SHI[3], Ru HUANG[1] & Yanqing WU[1,2*]

[1]*School of Integrated Circuits and Beijing Advanced Innovation Center for Integrated Circuits, Peking University, Beijing* 100871*, China;*
[2]*Wuhan National High Magnetic Field Center and School of Integrated Circuits, Huazhong University of Science and Technology, Wuhan* 430074*, China*

Received 23 January 2024/Revised 2 April 2024/Accepted 13 May 2024/Published online 27 May 2024

Abstract Two-dimensional (2D) transition metal dichalcogenide (TMDC) semiconductor materials exhibit extraordinary electrical properties, holding promise for the realization of next-generation complementary metal-oxide-semiconductor (CMOS) devices at ultimate scaling. However, constrained by effective device doping strategies, the hole mobility and device performance of tungsten diselenide (WSe_2) p-type transistors, especially monolayer chemical vapor deposition (CVD)-grown WSe_2, have not met expectations. In this paper, an effective performance enhancement of monolayer WSe_2 p-type transistor was achieved through a molecular doping strategy. Synthesizing monolayer WSe_2 directly on SiO_2 back-gated substrates and leveraging energy band alignment design, 4-nitrobenzenediazonium tetrafluoroborate (4-NBD) molecular dopant with a concentration of 10 mM was utilized to modulate the Fermi level position of monolayer WSe_2 for hole doping. The devices demonstrated a more than 98% increase in hole mobility, reaching up to 97 $cm^2 \cdot V^{-1} \cdot s^{-1}$ while maintaining the current on/off ratio of 10^8. Monolayer p-type WSe_2 transistors with 1 μm channel length exhibit a high drive current surpassing 176 $\mu A \cdot \mu m^{-1}$, exceeding previous CVD-WSe_2 devices with similar channel length. This straightforward and effective approach to improving the electrical performance of WSe_2 transistors paves the way for advanced logic technologies based on transition metal dichalcogenide semiconductors.

Keywords CVD-grown WSe_2, molecular doping, 4-NBD, p-type transistors, hole mobility

1 Introduction

Two-dimensional (2D) transition metal dichalcogenides (TMDCs) offer a wide range of tunable bandgaps and extraordinary electrical properties, rendering them highly attractive for various applications, especially in electronic devices [1,2]. Theoretical considerations suggest that 2D materials possess far superior mobility compared to silicon at extremely scaled thicknesses, presenting potential advantages for ultimate transistor scaling for advanced logic devices [3,4]. Recently, molybdenum disulfide, as the most typical n-type TMDC material, has made remarkable progress in wafer-scale material synthesis of chemical vapor deposition and device performance optimization [5–7]. To further promote advancement of 2D material complementary metal-oxide-semiconductor (CMOS) technology, p-type 2D TMDC transistor technologies with matched threshold voltage and device performance are very necessary and desired. Among the prime candidates for p-type transistor technologies, WSe_2 stands out as one of the best candidates due to its more balanced conduction and valence band edges to different work function metals and impressive hole mobility [8–10]. Nevertheless, previous studies have encountered challenges related to mobility degradation, particularly concerning scalable chemical vapor deposition (CVD) monolayer WSe_2 [11–14].

Controlled channel doping techniques offer a practical means to modulate the electrical properties of 2D transistors [15,16]. Different from the complex doping process technologies established in the traditional semiconductor industry, such as ion implantation and thermal diffusion, the ultrathin nature

* Corresponding author (email: xiongxiong@pku.edu.cn, yqwu@pku.edu.cn)

and expansive surface area of 2D materials make them sensitive to the surrounding environment and thus amenable to modulation of surface charge transfer doping. In the previous studies, substitution doping and chemical adsorption were reported frequently. Partial substitution of W atoms with Nb achieves p-type character, the doping process needs to be done during WSe_2 growth while it is easy to over-dop resulting in very weak gate dependence. Besides, electrostatic doping is the most commonly used doping technique in 2D device technology. However, the doping concentration of electrostatic doping is limited by the dielectric breakdown, and it also requires additional electrode terminals and power supply, presenting challenges in the miniaturization of transistor technology. Typically, gases with oxidizing characteristics like NO_x, H_2O, and O_2 have been utilized as doping agents to enhance p-type device performance, as reported in previous studies [13, 17]. However, physical adsorption gases rapidly desorb and revert to their original state under vacuum conditions, while chemical adsorption may alter the original band structure, leading to device performance or electrostatic control degradation [12–14, 18]. To achieve effective enhancement of p-type transistor performance, one promising method involves using redox-active molecules capable of integer electron transfer reactions with TMDCs as dopants, yielding more robust and non-destructive doping effect [19, 20].

In this study, we demonstrated an effective chemical doping approach for low-pressure chemical vapor deposition (LPCVD) direct-grown monolayer WSe_2 field-effect transistors (FETs) employing 4-nitrobenzenediazonium tetrafluoroborate (4-NBD) p-dopants. Validation of efficient surface charge transfer effects was achieved through Raman and X-ray photoelectron spectroscopy (XPS) spectral analyses. The field-effect hole mobility of WSe_2 transistors increased significantly from the pristine 49 to 97 $cm^2 \cdot V^{-1} \cdot s^{-1}$, marking a remarkable 98% enhancement under the doping concentration of 10 mM. Importantly, unlike the degradation in off-state current reported in previous studies [14, 18] due to chemical doping, this study achieved improvements in the off-state current while maintaining a high on/off ratio of up to 1.2×10^8. Moreover, a high drive current exceeding 176 $\mu A \cdot \mu m^{-1}$ was achieved on the WSe_2 transistors with a 1 μm channel length, surpassing previously reported monolayer CVD p-type WSe_2 devices with the same channel length [19, 21–23]. This strategy offers a straightforward and effective means to boost the electrical performance of 2D p-type WSe_2 transistors, showcasing great potential in fabricating 2D CMOS applications.

2 Results and discussion

Monolayer WSe_2 was grown by molten-salt-assisted LPCVD process using WO_2 and Se precursors on a silicon substrate covered by 10 nm SiO_2 grown by atomic layer deposition (ALD). During the growth, 100 sccm of Ar was introduced as the carrier gas and 3 sccm H_2 as the reducing gas to reduce WO_2 to WO_{2-x}. An additional potassium chloride (KCl) was added to WO_2 powder to further reduce the formation energy of WSe_2 growth, as depicted in Figure 1(a). The morphology of molten salt-assisted LPCVD monolayer WSe_2 and an optical microscope photograph of the as-grown monolayer WSe_2 are shown in Figure 1(b), with a single crystal domain size of 80 μm. Photoluminescence (PL) spectra in Figure 1(c) exhibit a strong photoluminescence peak at 764 nm as the excitation of direct bandgap, suggesting a pure phase of monolayer WSe_2 with a bandgap of 1.6 eV [24, 25]. To exclude the doping of KCl during the growth process, the high-resolution X-ray photoelectron spectroscopy spectrum in Figure 1(d) of Cl 2p and K 2p was measured, where no evident peak was observed at 198.3, 200.3, 292.7, and 295.5 eV, indicating no KCl residue in WSe_2 film during the LPCVD process.

A key feature of this study is that WSe_2 can be grown directly on SiO_2 substrates without any transfer process, indicating that the proposed method is compatible with silicon-based substrates, providing a feasible path for integrating two-dimensional materials into existing silicon-based electronic devices. The device fabrication process in this study follows the integration process flow as shown in Figure 2(a). All patterning processes use standard electron-beam lithography. The substrate is low-resistance silicon with 10 nm ALD-SiO_2 back-gate dielectric. The source/drain contact was metalized with 20/40 nm Pt/Au at a deposition rate of 0.1–0.3 Å$\cdot$ s^{-1}, following the lift-off process. Inductively coupled plasma (ICP) was used to etch and define the active region. To minimize organic residues during fabrication and reduce carriers scattering, the transfer-free channel and low-energy source-drain metal evaporation process are crucial steps in achieving high mobility transistors, as depicted in Figure 2(b).

The scanning electron microscope (SEM) image of the channel region in Figure 2(c) shows no apparent process chemical residues in the channel and source/drain contact areas, benefiting from the transfer-

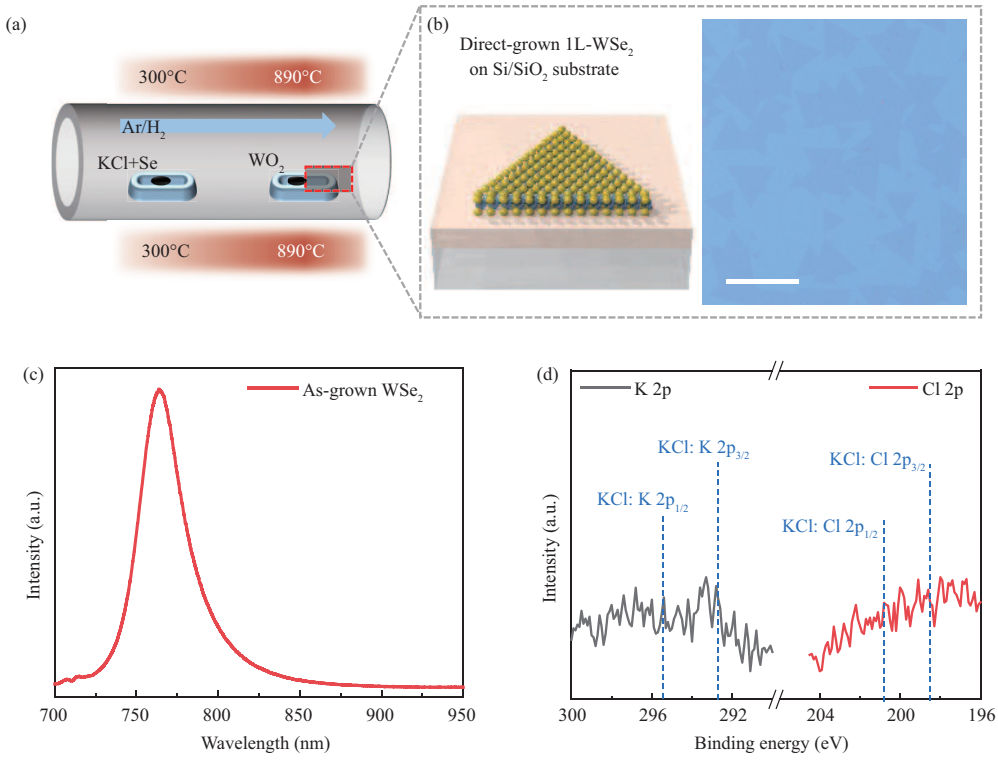

Figure 1 (a) Schematic of molten-salt-assisted LPCVD direct-growth of 1L-WSe_2 on Si/SiO_2 substrate; (b) schematic of 1L-WSe_2 structure on Si/SiO_2 substrate and corresponding optical micrograph of triangular grains (scale bar, 100 μm); (c) PL spectra of as-grown monolayer WSe_2; (d) high-resolution XPS spectra of Cl/K for as-grown WSe_2, the absence of Cl 2p and K 2p indicating no KCl residue in WSe_2 film during molten-salt-assisted LPCVD process.

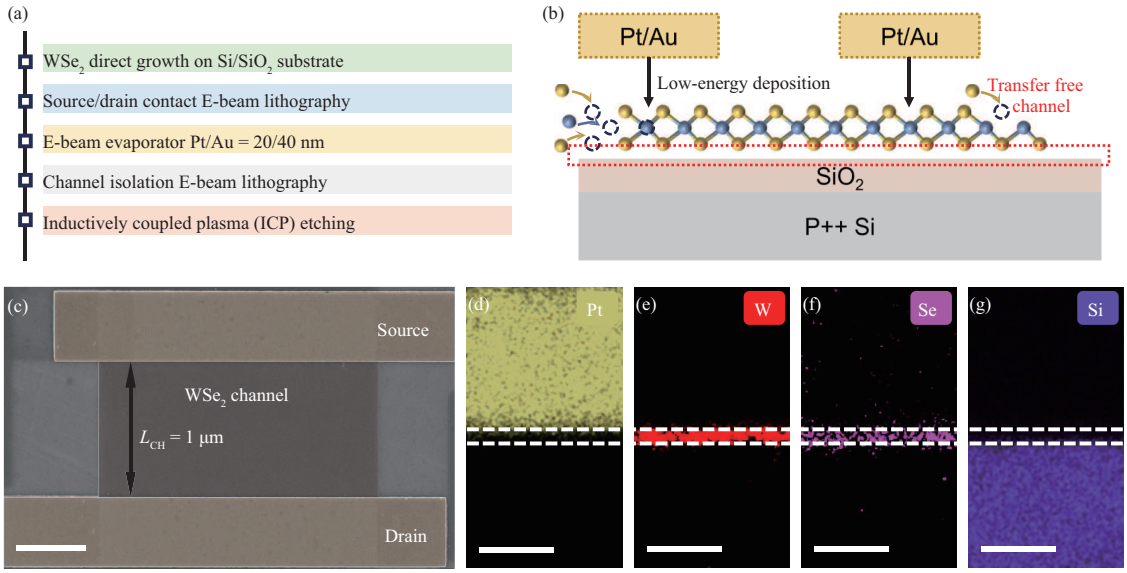

Figure 2 (a) Key process steps for fabricating WSe_2 transistors; (b) schematic of a transfer-free WSe_2 transistor with low-energy deposited Pt/Au contacts on a 10 nm SiO_2 dielectric; (c) SEM image of a WSe_2 transistor with a channel length of 1μm (scale bar, 500 nm); (d)–(g) cross-sectional EDX elements mapping of the contact region, detailing the interface of Pt contact and SiO_2 dielectric with monolayer WSe_2 channel (scale bar, 10 nm).

free channel material. A clean and sharp interface between contact metal and WSe_2 as well as back gate dielectric and WSe_2 is established due to the transfer-free WSe_2 channel and low-energy metal deposition. The energy dispersive X-ray spectroscopy (EDX) mapping of Pt, W, Se, and Si elements reveals the spatially resolved elemental distributions with an abrupt change across the neighboring films shown in Figures 2(d)–(g), further confirming the clear interfaces and absence of damage within the WSe_2

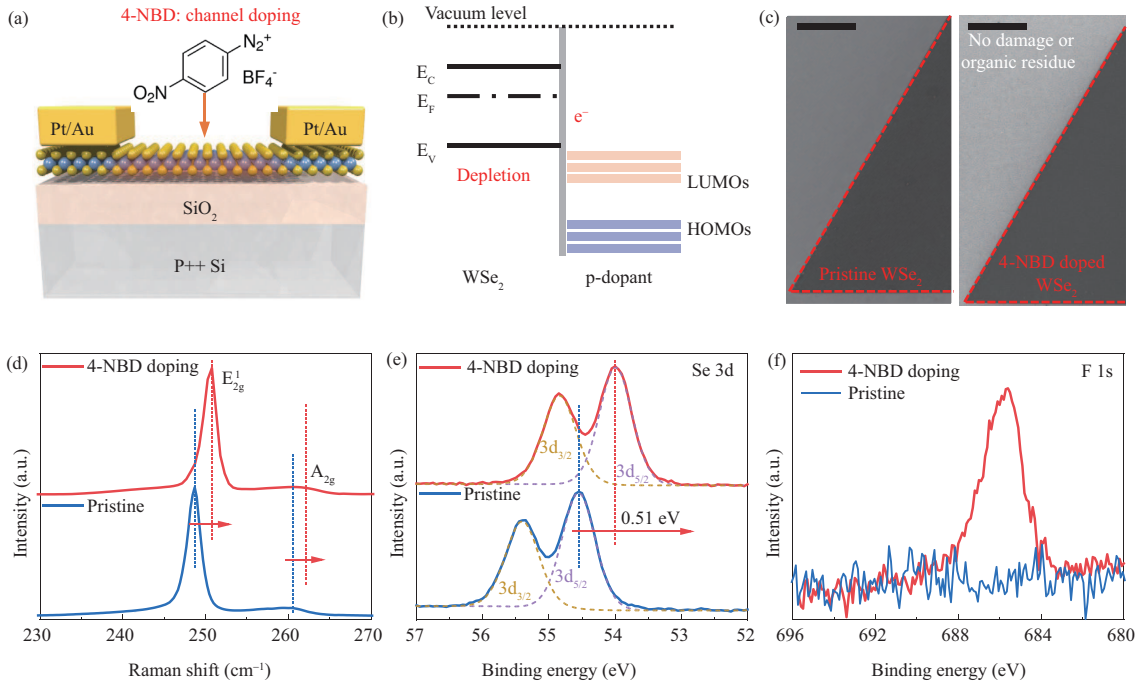

Figure 3 (a) Schematic view of 4-NBD channel doped 1L-WSe_2 transistor structure and chemical structure of 4-NBD; (b) band alignment of WSe_2 and 4-NBD p-dopant; (c) SEM images of pristine (left) and 4-NBD doped (right) WSe_2 (scale bar, 15 μm); (d) Raman spectra of 4-NBD doped and pristine WSe_2; high-resolution XPS spectra of Se 3d (e) and F 1s (f) for pristine and 4-NBD doped WSe_2.

film, all serving as the basis for achieving high mobility devices.

The subsequent molecular doping was performed on the back-gated WSe_2 devices, employing the selected 4-NBD molecular structure as illustrated in Figure 3(a). The fabricated WSe_2 FETs were immersed in an acetone solution of 4-NBD with concentrations of 10 mM and kept in solution for 10 min at room temperature without heating, following rinse in the isopropanol to wash off the supererogatory dopants. Figure 3(b) displays the energy levels of WSe_2 and 4-NBD [26]. The highest occupied molecular orbital energy of 4-NBD is lower than the valence band edge of WSe_2, which induces electrons from WSe_2 to 4-NBD, resulting in the p-doping in WSe_2. As depicted in Figure 3(c), SEM images displayed no discernible damage or organic residues during the WSe_2 doping process.

Raman spectroscopy and XPS were performed to further investigate the impact of surface charge transfer effect in 4-NBD doped WSe_2. Figure 3(d) shows the Raman spectrum (using a laser with the wavelength of 514 nm) of the pristine WSe_2 (blue curve), exhibiting the E^1_{2g} peak at 248.69 cm^{-1} and the A_{2g} peak at 260.53 cm^{-1}. A comparison with the spectrum of doped WSe_2 (red curve) revealed both peaks significantly shifted towards higher wavenumbers, indicating decreased electron-phonon scattering due to p-doping. The p-doping effect is also confirmed by XPS. The peak shape of the Se 3d core level shows no apparent changes, suggesting no chemical structure alterations or damage in the WSe_2 channel [26]. While the comparison of Se 3d core level doublet ($3d_{5/2}$ and $3d_{3/2}$) of pristine WSe_2 and 4-NBD doped WSe_2 in Figure 3(e) shows a 0.51 eV shift towards lower binding energy in the doped WSe_2. This shift is attributed to band bending in WSe_2 due to charge transfer from WSe_2 to 4-NBD, consistent with the Fermi level moving closer to the valence band [26]. Furthermore, the appearance of F 1s cole level in doped WSe_2 indicates effective doping of WSe_2, as shown in Figure 3(f).

The direct comparison of the electrical performance of the devices demonstrates the effectiveness of the doping effect. Figure 4(a) illustrates the transfer characteristics for pristine and doped monolayer WSe_2 transistors ($V_{DS} = -1$ V) measured under a vacuum environment of below 10^{-5} torr at room temperature. The pristine WSe_2 transistor exhibits p-type characteristics with an on/off ratio of $>10^6$ and an on-state current of 76 μA · $μm^{-1}$ at $V_{DS} = -2$ V. The pristine WSe_2 transistor did not exhibit n-type behavior under positive gate bias. The intrinsic high current of WSe_2 is a result of transfer-free processes, which mitigate the damage to WSe_2. After the introduction of 10 mM 4-NBD doping, the doped device shows a significant positive shift in threshold voltage while improving both the on-state and off-state current, exhibiting a high on/off ratio exceeding 10^8, over an order of magnitude enhancement.

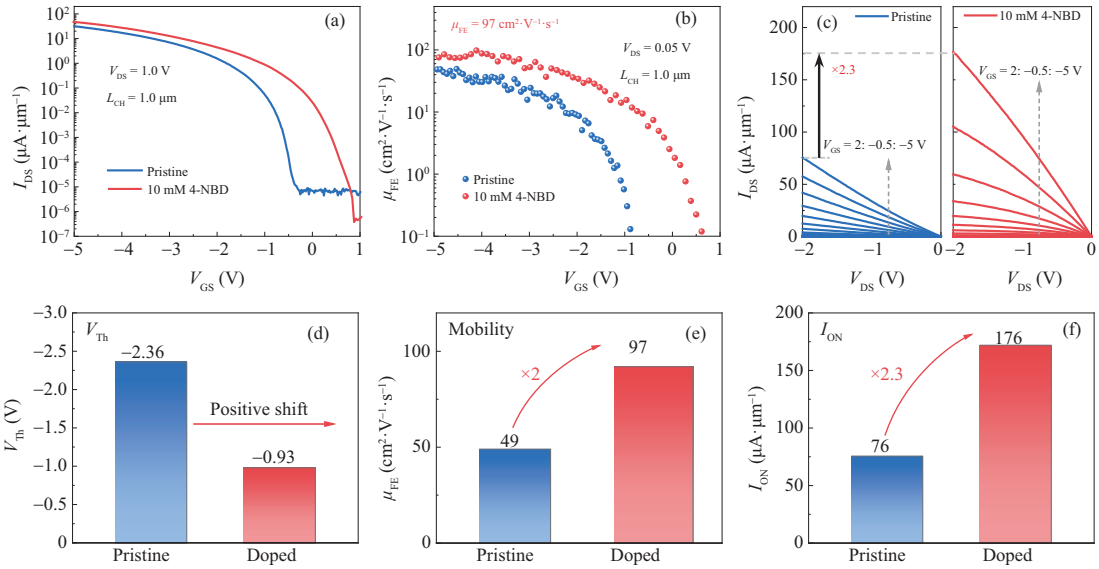

Figure 4 (a) Comparison of transfer characteristics of pristine (blue curve) and 10 mM 4-NBD doped (red curve) WSe_2 transistors with channel length of 1 μm and channel width of 1 μm at $V_{DS} = -1$ V; (b) field-effect mobility extraction of WSe_2 transistors at $V_{DS} = -0.05$ V; (c) output characteristics comparison of WSe_2 transistors with channel length of 1 μm (for the pristine WSe_2 FET, the range spans from $V_{GS} = 1$ to -5 V in steps of -0.5 V); (d) histograms of the threshold voltage shift from pristine to 10 mM 4-NBD doped WSe_2 FETs at $V_{DS} = -0.05$ V; histograms showing the optimization for 10 mM 4-NBD doped WSe_2 FETs of mobility ($V_{DS} = -0.05$ V) (e) and I_{ON} ($V_{GS} = -5$ V, $V_{DS} = -2$ V) (f), respectively.

Figure 4(b) presents the extracted field-effect hole mobility under low electric field conditions ($V_{DS} = -0.05$ V). The effective field-effect carrier mobility (μ_{FE}) was calculated by using

$$\mu = \frac{G_m L}{C_{ox} V_{DS} W}, \tag{1}$$

where $G_m = \mathrm{d}I_{DS}/\mathrm{d}V_{GS}$ as the transconductance obtained from the transfer curve at $V_{DS} = -0.05$ V; the C_{ox} is the capacitance per unit of the 10 nm thick SiO_2, the value of C_{ox} is 0.345 μF cm^{-2}; V_{DS} is the applied voltage of drain; L and W are the effective length and width of the channel. After the chemical doping process, the maximum carrier mobilities achieved by the 10 mM 4-NBD doped transistor is 97 cm^2 · V^{-1} · s^{-1}, which is over 98% higher than the pristine mobility of 49 cm^2 · V^{-1} · s^{-1}. Notably, the 10 mM 4-NBD doping significantly increases the hole mobility of WSe_2. The chemical doping increases the carrier concentration and reduces the influence of CVD-WSe_2 defects. Furthermore, the p-type doping reduces the contact resistance, thereby increasing the hole mobility [20, 26, 27]. Output characteristics of the transistors are shown in Figure 4(c); the blue and red curves are pristine and 10 mM 4-NBD doped transistors, respectively. The output drain current of the doped 1 μm channel length and 1 μm channel width reaches 176 μA · μm^{-1} at a drain bias of -2 V and gate voltage of -5 V, marking a 2.3-fold increase compared to the pristine WSe_2 transistors under the same bias voltage, far exceeding the most of previous studies such as NO_x doping [23], 2D contact [28], or novel metal contact for monolayer CVD p-type WSe_2 transistors [29–31]. Furthermore, the contact resistance is reduced from 8.64 to 5.86 kΩ · μm under the same carrier density after doping treatment by transmission line method (TLM), indicating an improvement of the metal-semiconductor interface. Figures 4(d)–(f) present a quantitative comparison of key parameters between the pristine WSe_2 field-effect transistor devices and 4-NBD-doped WSe_2 field-effect transistor devices, visually illustrating the performance enhancement brought about by doping. Figure 4(d) shows the positive shift from -2.36 to -0.93 V of threshold voltage at $V_{DS} = -1$ V due to the p-type doping of WSe_2. The effective field-effect carrier mobility and I_{ON} mark 2- and 2.3-times increase for 10 mM doped WSe_2 FETs, respectively, showing a significant improvement as shown in Figures 4(e) and (f). Advanced logic devices demand high on/off ratios and high mobility. The 10 mM 4-NBD doped WSe_2 device exhibits a high on/off ratio of 10^8 and a high hole mobility of 97 cm^2 · V^{-1} · s^{-1}, achieving high on-state current and extremely low off-state current (below 5×10^{-7} μA · μm^{-1}). Furthermore, Table 1 shows the comparison of the doped WSe_2 performance in this study with previous studies [26, 32], demonstrating the superiority of device mobility and on/off ratio in this study.

Table 1 Comparison of the doped WSe_2 performance

Ref.	Channel	Mobility ($cm^2 \cdot V^{-1} \cdot s^{-1}$)	On/off ratio	I_{ON} ($\mu A \cdot \mu m^{-1}$)	EOT[a)] (nm)
[32]	Solution-processed WSe_2	0.1	4×10^4	–	–
[26]	CVD-WSe_2 1L	82	1.0×10^7	–	90
This work	CVD-WSe_2 1L	97	1.2×10^8	176	10

a) EOT denotes equivalent oxide thickness.

3 Conclusion

In conclusion, we successfully demonstrated an effective chemical doping approach for LPCVD direct-grown monolayer WSe_2 FETs by employing 4-NBD p-dopants. The effectiveness of surface charge transfer was confirmed through comprehensive Raman and XPS spectral analyses. The field-effect hole mobility of WSe_2 transistors exhibited a significant increase from the initial 49 to 97 $cm^2 \cdot V^{-1} \cdot s^{-1}$, representing an impressive 98% enhancement under the 10 mM doping concentration. Importantly, unlike the degradation in off-current reported in previous literature due to chemical doping, this study achieved improvements in off-state current while maintaining a high on/off ratio of up to 10^8. Moreover, a high drive current exceeding 176 $\mu A \cdot \mu m^{-1}$ was achieved on the WSe_2 transistors with a 1 μm channel length. This strategy offers a straightforward and effective means to boost the PFET electrical performance of 2D WSe_2, showcasing great potential in fabricating 2D CMOS circuit applications.

Acknowledgements This work was supported by National Natural Science Foundation of China (Grant Nos. 61927901, 62090034, 62104012), National Key Research and Development Program of China (Grant Nos. 2022YFB4400102, 2021YFA1202903), Beijing Natural Science Foundation (Grant No. 4242057), and Technology Innovation Program of Hunan Province (Grant No. 2021RC5008).

References

1 Jeong J W, Choi Y E, Kim W S, et al. Tunnelling-based ternary metal-oxide-semiconductor technology. Nat Electron, 2019, 2: 307–312
2 Novoselov K S, Mishchenko A, Carvalho A, et al. 2D materials and van der Waals heterostructures. Science, 2016, 353: aac9439
3 Akinwande D, Huyghebaert C, Wang C H, et al. Graphene and two-dimensional materials for silicon technology. Nature, 2019, 573: 507–518
4 Radisavljevic B, Radenovic A, Brivio J, et al. Single-layer MoS2 transistors. Nat Nanotech, 2011, 6: 147–150
5 Xia Y, Chen X, Wei J, et al. 12-inch growth of uniform MoS_2 monolayer for integrated circuit manufacture. Nat Mater, 2023, 22: 1324–1331
6 Li W, Gong X, Yu Z, et al. Approaching the quantum limit in two-dimensional semiconductor contacts. Nature, 2023, 613: 274–279
7 Luo P, Liu C, Lin J, et al. Molybdenum disulfide transistors with enlarged van der Waals gaps at their dielectric interface via oxygen accumulation. Nat Electron, 2022, 5: 849–858
8 Ionescu A M, Riel H. Tunnel field-effect transistors as energy-efficient electronic switches. Nature, 2011, 479: 329–337
9 Akinwande D, Petrone N, Hone J. Two-dimensional flexible nanoelectronics. Nat Commun, 2014, 5: 5678
10 Liu W, Kang J, Sarkar D, et al. Role of metal contacts in designing high-performance monolayer n-type WSe_2 field effect transistors. Nano Lett, 2013, 13: 1983–1990
11 Yoon M, Lee J. Charge transfer doping with an organic layer to achieve a high-performance p-type WSe_2 transistor. J Mater Chem C, 2021, 9: 9592–9598
12 Tarasov A, Zhang S, Tsai M-Y, et al. Controlled doping of large-area trilayer MoS_2 with molecular reductants and oxidants. Adv Mater, 2015, 27: 1175–1181
13 Fang H, Chuang S, Chang T C, et al. High-performance single layered WSe_2 p-FETs with chemically doped contacts. Nano Lett, 2012, 12: 3788–3792
14 Yue D, Kim C, Lee K Y, et al. Ohmic contact in 2D semiconductors via the formation of a benzyl viologen interlayer. Adv Funct Mater, 2019, 29: 1807338
15 Luo P, Zhuge F, Zhang Q, et al. Doping engineering and functionalization of two-dimensional metal chalcogenides. Nanoscale Horiz, 2019, 4: 26–51
16 Zhao Y, Xu K, Pan F, et al. Doping, contact and interface engineering of two-dimensional layered transition metal dichalcogenides transistors. Adv Funct Mater, 2017, 27: 1603484
17 Liu B, Chen L, Liu G, et al. High-performance chemical sensing using Schottky-contacted chemical vapor deposition grown monolayer MoS_2 transistors. ACS Nano, 2014, 8: 5304–5314
18 Zhao P, Kiriya D, Azcatl A, et al. Air stable p-doping of WSe_2 by covalent functionalization. ACS Nano, 2014, 8: 10808–10814
19 Liu X, Qu D, Ryu J, et al. P-type polar transition of chemically doped multilayer MoS_2 transistor. Adv Mater, 2016, 28: 2345–2351
20 Tsai M Y, Zhang S, Campbell P M, et al. Solution-processed doping of trilayer WSe_2 with redox-active molecules. Chem Mater, 2017, 29: 7296–7304
21 Zhang S, Hill H M, Moudgil K, et al. Controllable, wide-ranging n-doping and p-doping of monolayer group 6 transition-metal disulfides and diselenides. Adv Mater, 2018, 30: 1806345
22 Kim J K, Cho K, Jang J, et al. Molecular dopant-dependent charge transport in surface-charge-transfer-doped tungsten diselenide field effect transistors. Adv Mater, 2021, 33: 2101598
23 Chiang C C, Lan H Y, Pang C S, et al. Air-stable p-doping in record high-performance monolayer WSe_2 devices. IEEE Electron Device Lett, 2022, 43: 319–322

24 Tonndorf P, Schmidt R, Böttger P, et al. Photoluminescence emission and Raman response of monolayer MoS_2, $MoSe_2$, and WSe_2. Opt Express, 2013, 21: 4908–4916

25 O'Brien K P, Dorow C J, Penumatcha A, et al. Advancing 2D monolayer CMOS through contact, channel and interface engineering. In: Proceedings of IEEE International Electron Devices Meeting, San Francisco, 2021

26 Ji H G, Solís-Fernández P, Yoshimura D, et al. Chemically tuned p- and n-type WSe_2 monolayers with high carrier mobility for advanced electronics. Adv Mater, 2019, 31: 1903613

27 McDonnell S, Addou R, Buie C, et al. Defect-dominated doping and contact resistance in MoS_2. ACS Nano, 2014, 8: 2880–2888

28 Li J, Yang X, Liu Y, et al. General synthesis of two-dimensional van der Waals heterostructure arrays. Nature, 2020, 579: 368–374

29 Cheng C C, Chung Y Y, Li U Y, et al. First demonstration of 40-nm channel length top-gate WS_2 pFET using channel area-selective CVD growth directly on SiOx/Si substrate. In: Proceedings of IEEE Symposium on VLSI Technology and Circuits, Kyoto, 2019. 244–245

30 Naylor C H, Maxey K, Jezewski C, et al. 2D materials in the BEOL. In: Proceedings of IEEE Symposium on VLSI Technology and Circuits, Kyoto, 2023. 1–2

31 Dorow C, O'Brien K, Naylor C H, et al. Advancing monolayer 2-D nMOS and pMOS transistor integration from growth to van der Waals interface engineering for ultimate CMOS scaling. IEEE Trans Electron Dev, 2021, 68: 6592–6598

32 Zou T, Noh Y Y. Efficient p-doping on solution-processed WSe_2 nano-flake thin-film transistors for flexible electronics. In: Proceedings of the 7th IEEE Electron Devices Technology & Manufacturing Conference (EDTM), 2023. 1–3